Long-lived isomers in neutron-rich $Z = 72$–76 nuclides

M. W. Reed,[1,2,*] P. M. Walker,[1,3] I. J. Cullen,[1] Yu. A. Litvinov,[4,5] D. Shubina,[4] G. D. Dracoulis,[2] K. Blaum,[4]
F. Bosch,[5] C. Brandau,[6,7] J. J. Carroll,[8] D. M. Cullen,[9] A. Y. Deo,[1] B. Detwiler,[10] C. Dimopoulou,[5] G. X. Dong,[11]
F. Farinon,[5] H. Geissel,[5,12] E. Haettner,[12] M. Heil,[5] R. S. Kempley,[1] R. Knöbel,[5] C. Kozhuharov,[5] J. Kurcewicz,[5]
N. Kuzminchuk,[5] S. Litvinov,[5] Z. Liu,[13] R. Mao,[14] C. Nociforo,[5] F. Nolden,[5] W. R. Plaß,[12] Zs. Podolyak,[1]
A. Prochazka,[5] C. Scheidenberger,[5,12] M. Steck,[5] Th. Stöhlker,[5,15] B. Sun,[16] T. P. D. Swan,[1] G. Trees,[10]
H. Weick,[5] N. Winckler,[4,5] M. Winkler,[5] P. J. Woods,[13] F. R. Xu,[11] and T. Yamaguchi[17]

[1]*Department of Physics, University of Surrey, Guildford, Surrey GU2 7XH, United Kingdom*
[2]*Department of Nuclear Physics, R.S.P.E., Australian National University, Canberra ACT 0200, Australia*
[3]*CERN, CH-1211 Geneva 23, Switzerland*
[4]*Max-Planck-Institut für Kernphysik, Saupfercheckweg 1, 69117 Heidelberg, Germany*
[5]*GSI Helmholtzzentrum für Schwerionenforschung, Planckstraße 1, 64291 Darmstadt, Germany*
[6]*ExtreMe Matter Institute EMMI and Research Division, GSI Helmholtzzentrum für Schwerionenforschung, Planckstraße 1,
64291 Darmstadt, Germany*
[7]*Institut für Atom- und Molekülphysik, Justus-Liebig-Universität, 35392 Giessen, Germany*
[8]*US Army Research Laboratory, 2800 Powder Mill Road, Adelphi Maryland, USA*
[9]*Schuster Laboratory, University of Manchester, Manchester M13 9PL, United Kingdom*
[10]*Youngstown State University, One University Plaza, Youngstown, Ohio 44555, USA*
[11]*Department of Technical Physics, Peking University, Beijing 100871, China*
[12]*II Physikalisches Institut, Justus-Liebig-Universität Gießen, 35392 Gießen, Germany*
[13]*School of Physics and Astronomy, University of Edinburgh, Edinburgh EH9 3JZ, United Kingdom*
[14]*Institute of Modern Physics, Chinese Academy of Sciences, Lanzhou 730000, China*
[15]*Physikalisches Institut, Universität Heidelberg, Philosophenweg 12, 69120 Heidelberg, Germany*
[16]*School of Physics and Nuclear Energy Engineering, Beihaug University, 100191 Beijing, China*
[17]*Graduate School of Science and Engineering, Saitama University, Saitama 338-8570, Japan*

A study of neutron-rich isotopes in the $A = 185$ region of the nuclear chart has uncovered long-lived (>1 s) isomers in several isotopes of hafnium, tantalum, tungsten, rhenium, and osmium. The region was accessed via the use of projectile fragmentation with the UNILAC-SIS accelerators at GSI. Fragmentation products of ^{197}Au were passed through the fragment separator (FRS) and injected into the experimental storage ring (ESR), where single-ion identifications could be made. Evidence is presented for isomers in ^{183,184,186}Hf, ^{186,187}Ta, ^{186}W, ^{190,192,194}Re, and ^{195}Os with excitation energies in the range of 0.1–3.0 MeV. The lightest of these nuclides have well deformed prolate shapes, while the heaviest are transitional and susceptible to shape changes. Their properties are interpreted with the help of multi-quasiparticle and potential-energy-surface calculations.

I. INTRODUCTION

The neutron-rich region of the nuclear chart, with A = 180–190, is understood to be favorable for the creation of high-energy long-lived isomers, due to the nuclear shape and underlying shell structure [1,2]. Highly excited isomeric states occur in deformed nuclei when nucleon pairs can be broken and recoupled, with minimal energy cost, to high spin, resulting in yrast traps [2]. Specific predictions for the $Z = 72$ hafnium isotopes [2–4] indicate a continuation of the well known [5] isomer-rich stable nuclides far into the neutron-rich region. Indeed, there is the possibility that a case analogous to the 31-yr, 2.446-MeV isomer in ^{178}Hf [6] could exist in ^{188}Hf [2,4,7], with eight neutrons more than the heaviest stable isotope. However, shape calculations performed for neutron-rich nuclei in this mass region show increasing

gamma softness and a prolate-oblate shape change [8,9] close to $N = 116$. Such a shape instability could dramatically reduce the decay-transition hindrance factors and shorten the isomer lifetimes. Nevertheless, configuration-constrained potential-energy-surface (PES) calculations [4] indicate that (approaching ^{188}Hf) although the ground state might be gamma soft or triaxial, the prolate shape is stabilized for high-K excited states, keeping the possibility that high-K configurations will remain isomeric. The study of neutron-rich nuclei in this mass region may therefore give access, through isomer formation and decay, to the predicted prolate-oblate shape transitional nuclides.

Conventional methods such as fission or fusion-evaporation reactions are generally limited in their ability to reach heavy neutron-rich isotopes, whereas projectile fragmentation provides a convenient tool to access these nuclei [10]. The additional capability with relativistic fragmentation to identify projectile-like reaction products, on an ion-by-ion basis, enables ion selection in experiments and unique Z and

A identification. This is largely due to the fragment ions, in the main, being fully stripped of atomic electrons. To date, projectile fragmentation in combination with in-flight fragment separation has enabled microsecond isomers to be found some distance from the line of stability [11–13], through the emission of time-correlated gamma rays. The detection of long-lived isomers however, is not possible with that technique. Nevertheless, with the experimental storage ring (ESR) it is now feasible to directly observe an isomer without necessarily detecting its decay [14]. The ESR enables observation of single ions, allowing measurements to be performed despite very low production cross sections [15], with the ability to measure excitation energies of states with half-lives greater than 1 s. This experimental technique can thus be used to complement the well established γ-ray methods.

Using the fragment separator (FRS) [16], and a reaction involving removal of (sometimes many) nucleons from a parent beam of ^{197}Au it was possible to access the region of interest. The highest-spin isomer observed to date in fragmentation is the known $43/2\,\hbar$ state in ^{215}Ra [17,18]. Therefore, experimentally, access to states with spins up to $\sim 20\hbar$ can be expected. Highlights of the present work have recently been published in Ref. [19].

II. EXPERIMENT

The ESR is a heavy-ion storage ring [20] which is used to store, measure and accumulate ions produced in reactions on stable ions accelerated by the heavy-ion synchrotron (SIS). A maximal bending power of the ESR dipole magnets is 10 Tm, which corresponds for bare uranium ions to about 500 A MeV [20,21]. The ESR cooling system allows for both electron cooling [22] and stochastic precooling [23] to be performed on injected ions. Due to the nuclear reaction process there is an inevitable velocity spread for the injected ions which prevents unambiguous particle identification. Therefore a reduction in the initial injected ion velocity spread is required, this is performed by the process of "cooling." The revolution frequencies of cooled ions reflect directly the mass-over-charge ratios of the ions, which is the basis of the Schottky mass spectrometry (SMS) technique [24,25]. Cooling reduces the velocity spread to $\Delta v/v \sim 10^{-7}$ when less than 1000 ions are injected [26]. The time required to reduce the velocity spread of the injected ions (cooling) is dependent on the original velocity spread of the injected ions and cooling technique. An essential parameter is the difference between the electron and ion velocities [27]. For a cocktail beam, the velocity of cooler electrons can be optimized for a specific ion species. Still a few seconds are required to cool down the initial velocity spread of the ions. Furthermore, moving to other ion species, the mean velocity of the ions changes, thus increasing the mismatch between ion and cooler electron velocities. This leads to substantially longer cooling times which can reach a few minutes. Cooling times can be significantly reduced when electron cooling is used in combination with stochastic precooling. With this setup a minimum time of ~ 1 s can be obtained, leading to a lower limit on the lifetime of ions measured with SMS [28]. Measurement times can be further

reduced if the ESR is operated in isochronous mode [25]. Although this is not discussed here, many examples can be found in the literature [29,30].

For this experiment the ^{197}Au beam was accelerated to energies of 478–492 A MeV (dependent on the specific products required) and impinged on a 1035(1) mg cm^{-2} Be target. For extra electron stripping, a 223(1) mg cm^{-2} niobium backing was added to the target. The reaction fragments were then selected using the FRS [16] with a 200-μm aluminium energy degrader installed at the second focal plane of the FRS. This enabled *Z* selection for ions traversing the FRS via energy loss in the degrader. This degrader was primarily employed to avoid injection of intense primary beam ions in different atomic charge states into the ESR. The selected ions were then injected into the storage ring and cooled via stochastic precooling and electron cooling, ready for analysis.

Stochastic cooling operates at a fixed ion energy of 400 A MeV. Cooled ions were measured using time-resolved SMS [31]. Measurements of ion revolution frequencies are directly proportional to the mass-over-charge ($\frac{m}{q}$) ratio of the cooled ions. The revolution frequency of the ions at this energy is ~ 2 MHz. At each revolution, every ion induces a tiny signal on two electrostatic plates, "Schottky pickups," installed inside the ESR vacuum. Details of the Schottky pickups can be found in Refs. [32,33]. The Fourier transform of the signal from the pickup yields a noise-power density spectrum, or "Schottky frequency spectrum." In this experiment the 30th harmonic revolution frequency was analyzed [15,34]. The choice of the harmonic number is defined by the resonant circuit system which can be operated at 30 or 60 MHz [35]. A frequency acceptance of around 320 kHz is given at the 30th harmonic. This is sufficient for measurements of a large range of nuclei around the ion of interest. To achieve digitization and a time stamp for each event the signal needs to be down-converted from around 60 MHz to a bandwidth of 0–320 kHz. This is performed by subtracting a local oscillator frequency from the original raw frequency via an image-rejector mixer. Full details can be found in Refs. [33,35,36]. In the following, all figures showing ESR frequency are relative to the 30th resonant harmonic (~ 60 MHz). The integrated noise power of a frequency peak is proportional to the corresponding number of stored ions. The variation of noise power with time provides information on the lifetime.

The experiment was split into three isotope and charge-state settings, such that the FRS-ESR system was optimized for a specific isotope. The SIS ion energy was tuned so that the investigated ion had an energy of 400 A MeV after the 200-μm aluminium degrader. For the ^{190}W setting, injections into the ESR were every 30 s, whereas for the ^{184,186}Hf settings, ions were injected every 60 s, with the option of delaying subsequent injections if an ion of interest appeared during online analysis. The online monitoring was performed with a real-time spectrum analyzer (RSA) providing fast Fourier transform (FFT) spectra with a narrow bandwidth, concentrated on the isotope of interest. The data were also stored offline so that a complete spectrum analysis could be performed subsequently. With stochastic precooling optimized for the isotope of interest, other injected ions (which have significantly different values of m/q) may experience cooling

times that are much longer than those for the isotope of interest. The stochastic precooling was operated for about 1 s. This mechanism cools ions in a limited frequency bandwidth [23]; ions lying outside this cooling bandwidth are effectively heated, which leads to longer electron-cooling times. This "slow" cooling limits the observation time of ions which fall outside the cooling bandwidth. An ion measurement is dependent on the ion lifetime, cooling time, and measurement time.

In a single injection from the SIS-FRS many different ion species are stored. Some of these nuclides may have well known masses and can thus be used to calibrate the frequency spectra. As the first step, the momentum compaction factor (α_p) of the ring is known to an approximate degree from the magnetic rigidity of the ring setup [24,37]. Furthermore, the frequency differences in an observed isobaric chain offer a unique finger-print of m/q ratios, which in combination with α_p, aids in ion identification. The strong peaks in the spectrum are likely to be those near the mass of the primary beam. By initially identifying the strong peaks, mass tables [5] can be used to identify the peaks at higher and lower frequencies. In this way it is possible to identify all the ion species measured in the ESR [38].

III. RESULTS

A. Atomic electron capture and stripping

Atomic electron capture (aec) and stripping can play an important role in the measurement of ion lifetimes in the ESR. Atomic electron capture occurs mainly in the electron cooler. The ESR is an ultrahigh vacuum machine with a rest gas pressure in the 10^{-11} mbar range and with H_2 being the main rest-gas component. The experiment was performed at high energy (400 A MeV); therefore, electron capture from the residual gas can be neglected. However, the stripping of electrons from stored hydrogen- or helium-like ions can occur by collisions with the residual gases. It is important to measure the effect as the lifetime is vacuum and electron cooler current dependent and cannot be easily calculated. The lifetime for atomic electron capture scales as Z^2 for different ions [36], such that

$$\tau_{aec(Z_2)} = \tau_{aec(Z_1)} \frac{(Z_1)^2}{(Z_2)^2}. \tag{1}$$

By measuring integrated Schottky noise power at different times, a lifetime for a peak can be measured. In Fig. 1, the red data points are measurements for stable helium-like ^{196}Pt. The apparent decay is due to losses from the ion orbit by either atomic electron pick-up or stripping. An observed in-ring survival half-life of 26(3) min has been measured for this ion. For ions with one or more electrons in an atomic shell the loss mechanism is a combination of electron stripping and atomic electron capture [36].

The most exotic ions observed in the ESR however, are not in helium-like or hydrogen-like charge states but are seen as bare ions. The most populated bare ion is ^{194}Os^{76+} in the present measurement. Due to its long nuclear half-life of 6 yr [39], the radioactive decay can safely be neglected for our
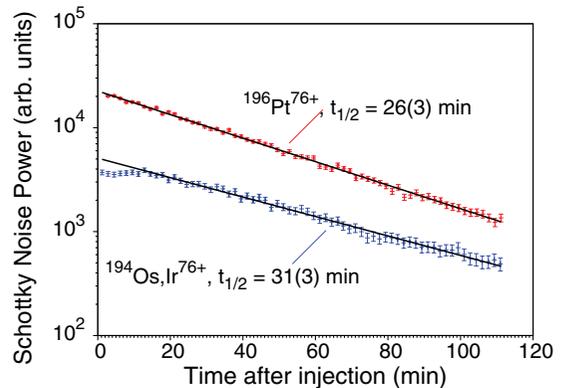
FIG. 1. (Color online) Measured survival curves for highly charged ions (helium-like, hydrogen-like, and bare) in the ESR. The curves show in-ring survival times (i.e., not Lorentz corrected). The flattening in the lower curve is due to feeding of the peak by electron stripping of the hydrogen-like ^{194}Os^{75+} and helium-like ^{194}Ir$^{m,g,75+}$ less populated charge states.

short measurement times and thus this ion can be classed as "pseudostable." However, since it is very close in mass excess to other pseudostable ions of ^{194}Ir$^{m,g,76+}$, their different masses cannot be resolved. Measurements were taken for the entire unresolved peak and the results are shown in Fig. 1 (blue data points). The fitted curve shows a survival half-life of 31(3) min in the ESR for the entire peak. It is expected that, if two significantly different lifetimes were present, these would be observed in the lifetime curve. However, two curves cannot be distinguished, suggesting that bare and hydrogen-like ions have a similar survival half-life.

To check this result after correction for Z^2 dependence, two other bare ions have been analyzed, ^{190}W^{74+} and ^{184}Hf$^{g,72+}$, although with much lower statistics. Partial half-lives need to be considered for ^{190}W and ^{184}Hf^g as both have nuclear decays that could contribute to losses from the ring. For ^{190}W^{74+}, four decays were observed in an observation time of 6040 s, leading to a Lorentz-corrected mean lifetime of $18.0^{+13.6}_{-9.1}$ min, and a measured half-life of $12.6^{+9.4}_{-6.3}$ min. This is significantly lower than the β-decay half-life of 30.0(15) min [40]. Atomic electron capture presumably contributes to the additional losses. Using the known β decay half-life and analysis of partial lifetimes, an in-ring survival half-life of 30^{+21}_{-15} min is found for ^{190}W^{74+}. A similar analysis was used on ^{184}Hf. In that case four decays were observed in a total time of 5820 s; leading to an overall mean in-ring life-time of 24^{+18}_{-12} min. Analysis with partial half-lives gives an atomic in-ring survival half-life of 18^{+14}_{-9} mins. Both measured bare survival half-lives (within error bars) are similar to the 31(3) min measured value for ^{194}Os, which suggests that this result is reliable.

B. Isomer results

Many new isomers in neutron-rich heavy atomic nuclei have been discovered and new information obtained on known isomers. It has been possible to extract excitation energies for all the isomeric states, and in some cases, half-lives (see Table I). Regarding the identification of isomers by this

TABLE I. Measured and calculated isomeric energies, half-lives, spins, and parities. The ground-state spin and parities are also shown. Isomers measured for the first time in this work are indicated in bold font. When ">" is shown for the number of ions, this indicates that either the number of ions could not be determined (^{192}Re) as the isomer and ground state become unresolvable when injected together and thus a lower limit is shown, or the analysis was curtailed (^{186}W) as many ions were observed and more identifications would not yield greater accuracy. For ^{190}Re, it is be a combination of both.

Ion	No. of ions	E^*_{ESR}	E^*_{calc} (keV)	K^π	$t_{1/2}$[a] (decay mode)	β/γ[b]
^{183}Hf$^{g,71+}$	30	0	0	$(3/2^-)$	1.07(2) h [5] (β)	
^{183}Hf$^{m,71+}$	1	1464(64)	1712	$(27/2^-)$	10^{+48}_{-5} s (γ)	
^{184}Hf$^{g,72+}$	86	0	0	0^+	4.12(5) h [5] (β)	
^{184}Hf$^{m1,72+}$	32	1264(10)	1241	(8^-) [41]	113^{+60}_{-47} s (β, γ)	3/4
^{184}Hf$^{m2,72+}$	20	2477(10)	2369	(15^+)	12^{+8}_{-6} min (β)	
^{186}Hf$^{g,72+}$	8	0	0	0^+	2.6(12) min [5] (β)	
^{186}Hf$^{m,72+}$	2	2968(43)	2269	(17^+)	>20 s	
^{186}Ta$^{g,72+}$	120	0	0	[c]	10.5(3) min [42] (β)	
^{186}Ta$^{m,72+}$	60	336(20)			$3.0^{+1.5}_{-0.8}$ min (β, γ)	2/5
^{187}Ta$^{g,73+}$	102	0	0	$(7/2^+)$	2.3(6) min (β)	
^{187}Ta$^{m1,73+}$	17	1793(10)	1508	$(27/2^-)$	22(9) s (β, γ)	5/8
^{187}Ta$^{m2,73+}$	9	2933(14)	2710	$(41/2^+)$	>5 min $((\beta))$	
^{186}W$^{g,72+}$	>100	0	0	0^+	stable	
^{186}W$^{m,72+}$	5	3560(59)		(16^+) [43]	$7.5^{+4.8}_{-3.3}$ s (IC)	
^{190}Re$^{g,74+}$	>40	0	0	(2^-) [42]	3.1(3) min (β) [5]	
^{190}Re$^{m,74+}$	>60	204(10)		(6^-) [42]	3.2(2) h (γ) [5]	
^{192}Re$^{g,75+}$	>40	0	0		16(1) s (β) [5]	
^{192}Re$^{m,75+}$	>27	267(10)			61^{+40}_{-20} s (γ, β)	2/9
^{194}Re$^{g,75+}$	1	0	0		5(1) s (β) [44]	
^{194}Re$^{m1,75+}$	1	285(40)			25(8),100(10) s (β) [44]	
^{194}Re$^{m2,75+}$	2	833(33)			25(8),100(10) s (β) [44]	
^{195}Os$^{g,76+}$	63	0	0	$(3/2^-)$	$\sim$ 9 min (β) [12]	
^{195}Os$^{m,76+}$	73	454(10)			>9 min $(\gamma, (\beta))$	(1)/1

[a]In all cases the ion is in a high charge state (bare, H-like, or He-like) and the quoted lifetime is for that charge state. In the case of ground-state decay this should have no effect as the decay is via β^-. However, in the case for excited states, internal conversion can be hindered (in the case of H-like, He-like) or stopped entirely (bare) extending the lifetime. As spectroscopic information is not available, the effect of this hindrance cannot be determined.

[b]The branching ratio shown is β/γ and not β/internal decay.

[c]See Sec. IV D.

technique, sometimes there can be an ambiguity between a potential isomer and a less-bound isobar. For example, an isomer in ($Z = 72$) Hf could be interpreted as the ground state of ($Z = 71$) Lu, if the mass of the latter were otherwise unknown. However, using SMS, this scenario is rigorously excluded in many cases, by exploiting the option of observing the bare ion of the isobar of interest; e.g., if the Hf ion is *bare*, with $q = 72+$, then the Lu isobar is excluded. In principle, in this case, a higher-energy isomer of the Ta isobar could also account for these ions. This interpretation is generally not considered further for high-energy isomers, as it is thought to be unlikely in most cases that arise in the present study, as higher energy and spins are unlikely to be accessed or observed in the experiment. In the cases for the low-energy isomers, these are either known from previous spectroscopy experiments or observed to γ decay in the present experiment, ruling out the possibility of the higher-energy isomer.

The experiment was split into three mass and charge state settings: ^{190}W^{74+}, ^{184}Hf^{72+}, and ^{186}Hf^{72+}. The ^{190}W setting had, for the most part, short observation times of 30 s per

injection (no long-lived isomer was observed in this nuclide). The ^{184}Hf setting had observation times of around 1 min, with injections occasionally being stopped to observe candidate isomers for longer periods. The third setting was intended to be centered on ^{186}Hf and, as in the previous case, injections were stopped for longer periods. However, subsequent offline analysis found the online determination to be incorrect, due to a misidentification. The online monitoring was in fact not focused on the frequency window corresponding to ^{186}Hf, but on a 6 kHz band which included ^{189}W^{74+} and ^{194}Au^{76+}. Thus the isomer in ^{186}Hf subsequently identified in offline analysis was not examined for longer periods.

Typically, in an individual injection, a single ion (at most) of a given exotic nuclide is observed. Therefore, conventional decay-curve analyses cannot be performed. By measuring single ions over the course of an injection and summing the observation time for all ions a total observation time can be found. The total number of measured decays in that time allow a mean lifetime to be estimated. This can then be Lorentz-corrected and a half-life calculated. However, for low
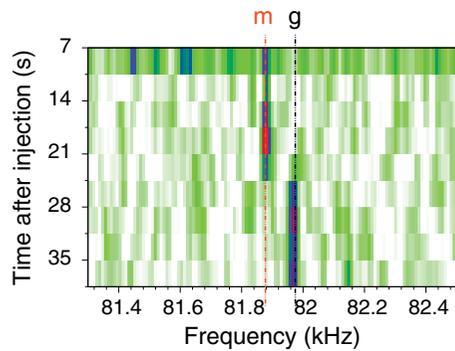
FIG. 2. (Color online) γ-decay event of an isomer observed in ^{183}Hf. Color code represents the Schottky noise power density in arbitrary units.

statistics, the error estimation of $\Delta = \sqrt{n}$ does not hold [45], where n is the number of measurements. Therefore, errors were analyzed using the methodology presented in Ref. [45].

C. ^{183}Hf

A γ-decaying isomer in ^{183}Hf was identified with the ^{184}Hf ESR experimental setting. The statistics for this isotope are very low, with only 30 ground state ions being observed in the ESR. A single ion was observed in the isomeric state, with a γ decay after $\sim$25 s to the corresponding ground state. Such a γ-decay event causes a sudden shift in ion frequency, as seen in Fig. 2.

With this isomer there is also a possible ambiguity in the identification; since the ^{183}Hf ions are hydrogen-like, a higher-mass isobar of fully stripped ^{183}Lu^{71+} could occur in the same region. However, this possibility can be dismissed by examining the frequency difference between the proposed isomer and the ground state of ^{183}Hf. The frequency difference is too small to account for the expected variation in mass between the two isobars. Furthermore, the sudden frequency change during the observation period is only compatible with a γ decay.

The measurement and associated error for the excitation energy was found using a reference peak (^{188}W^{73+} at $\sim$ 90 kHz) to calculate the difference in frequency between the ground state and the isomer (at $\sim$82 kHz). The frequency difference cannot be measured directly (unless both isomer and ground state are in the same injection) as there can be small but significant frequency shifts with respect to the original injection frequency, due to stochastic changes in the strengths of the produced magnetic fields. However, these shifts are the same for every stored ion and have been studied rigorously in Ref. [46], and by measuring frequency differences with respect to a reference line the shifts can be removed. The error in each measurement is calculated using the standard deviation of the frequency difference from the mean value. The average frequency difference between ground state and isomer is then calculated with the errors summed in quadrature. The average frequency difference can be used in conjunction with another calibration peak (of known mass) to determine the difference in mass-to-charge ratio between the ground state

and isomer, which is subsequently converted into an energy difference. In this case ^{183}Ta (together with ^{188}W) is used. The errors on the masses of ^{183}Ta and ^{188}W do not contribute significantly. By changing the mass of either ^{183}Ta or ^{188}W by 1σ, the measured mass of ^{183}Hf^g and ^{183}Hf^m will shift by the same amount. Thus the difference in mass between the isomer and ground state is unaffected. In general, this is only true when the frequency differences between the measured ions is small relative to the calibration range, as is the case for all isomers. Only the precision of the centroid determination contributes significantly to the final error. This principle was used to measure the energy of all the isomers discussed in this paper. Reference masses have been obtained from Ref. [5], unless otherwise stated.

In Fig 2, the isomer is the ion trace at the lower frequency. The sudden shift in frequency at $\sim$25 s is due to the spontaneous γ decay of the ion. All other ion traces in the full range of data (not shown in the figure) do not show such a jump. The ^{183}Hf isomer has been measured to have an excitation energy of 1.464(64) MeV, with a half-life of $t_{1/2}^{71+} = 10^{+48}_{-5}$ s.

The error determination for the energy of an isomer is not only dependent on the number of ions measured in the ESR but also the length of time those ions were observed. By dividing the measurement time into bins of $\sim$10 s, it is possible to gain good background reduction such that a peak can be well resolved. The measurement of the isomer in ^{192}Re (see Sec. III J) yielded an error bar of $\sim$10 keV, which was from 45 measured time bins, whereas, the measurement of 1.464(64) MeV for ^{183}Hf was gained by measuring only three, $\sim$3 s time bins.

D. ^{184}Hf

In the online analysis it was possible to view the $A = 184$ isobaric region in real time. A long-lived [48(10) s] γ-decaying, $K^\pi = 8^-$ isomer at 1.272(1) MeV was known in ^{184}Hf from earlier work [41] and its observation here serves as a convenient check on our ion identification and decay observation. A total of 32 ^{184}Hf$^{m1,72+}$ ions were observed, seven of which decayed. Of the decay events four were γ decays and three were lost from the ring, presumably β-decay events. Figure 3 illustrates one γ decay and one β decay. We note that β decay was not previously identified as a decay mode from this isomer. This is a bare nucleus, therefore internal conversion is not possible, although the neutral-atom internal conversion coefficient for the 555-keV $M2$ transition that depopulates the isomer [41] is low ($\sim$0.1 [47]), so the neutral-atom and bare-ion half-lives should be similar. The measured half-life of $t_{1/2}^{72+} = 113^{+60}_{-47}$ s is within 2σ of the previously measured value of 48(10) s. The excitation energy of 1.264(10) MeV measured in the ESR matches (within errors) the more accurate, previously published, result.

A second higher-lying isomer was observed in the ESR (Fig. 3); in total twenty ^{184}Hf^{m2} ions were observed, and on five occasions the subsequent injection was delayed so that an extended measurement of a single ion could be performed (Fig. 3). In four of the cases, the observed ion was lost from the ESR, at 4, 9, 11, and 18 min. For the final stopped injection

FIG. 4. (Color online) An isomer in ^{186}Hf. The red and blue lines show data from different injections. Using ^{186}W as a reference the isomer is clearly separate from the ground state.

because of the $q = 72+$ constraint. The data give a measured excitation energy of 2.968(43) MeV for the isomer (if the ion were an isomer in ^{186}Ta then the measured excitation energy would be ~ 5150 keV). (The reference ions used for the energy measurement were ^{186}W^{72+} and ^{191}Re^{74+}.) A definite life-time was not obtained as neither of the two observed ions decayed during the measurement so that a limit of $t_{1/2}^{72+} > 20$ s is associated with this isomer. In comparison with ^{184}Hf, it is surprising that a lower-energy (~ 1.5 MeV) two-quasiparticle isomer was not observed. This is possibly due to poor statistics, or to such a state having a shorter half-life than the range of the present measurements ($t_{1/2}^{72+} < 10$ s). The latter is shown to be a possibility due to the systematic decrease of the 8^- lifetime across the isotopic chain from the $A = 180$ isotope (Table II).

F. ^{186}Ta

Evidence for a β-decaying isomer in ^{186}Ta with a half-life of 1.54(5) min had been reported previously, but without an associated excitation energy [49]. To avoid complications of beam crystalization [15] and poor frequency resolution, the techniques discussed in Ref. [50] have been used for all low-energy (<500 keV) isomers. Figure 5(a) shows frequency differences between an ion trace and the ^{194}Pt^{75+} reference, where each count represents an independent frequency centroid-difference determination. A strongly populated state is observed with a smaller frequency difference than that of the ground state of ^{186}Ta. This is the proposed isomer in ^{186}Ta with an energy of 336(20) keV. The references used

TABLE II. Known $K^\pi = 8^-$ 2QP isomers in $170 \leqslant A \leqslant 184$ Hf isotopes [41,60–66].

Ion	Energy(MeV)	$t_{1/2}$
^{170}Hf	2.184	23(2) ns
^{172}Hf	2.006	163(3) ns
^{174}Hf	1.798	2.39(4) μs
^{176}Hf	1.559	9.9(2) μs
^{178}Hf	1.147	4.0(2) s
^{180}Hf	1.142	5.47(4) h
^{182}Hf	1.173	61.5(15) min
^{184}Hf	1.272	48(10) s

FIG. 3. (Color online) Observation of $q = 72+$ ions of ^{184}Hf and ^{184}Ta over three injections [Fig. 3(a)]. A new injection is seen as a horizontal trace which represents yet uncooled ions. Three different states can be observed in ^{184}Hf: two isomeric and one ground state. Details of the third injection are shown in Fig. 3(b); two ^{184}Hf^{m1} ions were originally injected, however after the first ~ 10 s one ion γ decays into the ground state. Two minutes later, the second ion is lost from the ESR presumably as a β decay.

the isomeric ion was observed for 27 min with no loss from the ESR before the following injection was made. None of the ions was seen to γ decay, and all decaying ions were lost from the ESR. Five decays of ^{184}Hf^{m2} were observed in a total observation time of 5010 s, giving an observed mean lifetime of 1002 s. A measured half-life of $t_{1/2}^{72+} = 12^{+8}_{-6}$ min was obtained for the isomer, once atomic electron pick-up had been accounted for. The excitation energy for the state has been measured as 2.477(10) MeV (the reference ions used for both ^{184}Hf isomers were ^{184}Hf$^{g,72+}$ and ^{191}Re^{75+}).

E. ^{186}Hf

The most neutron-rich hafnium isotope studied in the present work is ^{186}Hf. Its ground state β decays with a half-life of 2.6(12) min [48] but no excited states have been reported. We now find evidence for an isomeric state (see Fig. 4). Although the statistics for the $A = 186$ isobaric region are poor due to slow cooling and the small production cross section, a high-lying isomer has been found through the observation of two ions. These cannot be from ^{186}Lu (or a ^{186}Lu isomer)

FIG. 5. (Color online) Data for the $A = 186$, $73 \leqslant Z \leqslant 75$ isobars (a) and the γ and possible β decays of ^{186}Ta^m (b).

for the energy measurement were ^{186}W^{72+} and ^{191}Os^{74+}. In the present experiment both β (or internal conversion, as discussed later) (three events) and γ (five events) decays have been observed [Fig. 5(b)], whereas previously only β-decay events were measured. Figure 5(b) shows two decays of the isomer in ^{186}Ta. Two ions of the isomer are injected into the ESR. After about 80 s, there is a loss from the ESR of one of the ions. It is not seen in the ^{186}Ta ground-state trace and therefore can be attributed to a β decay or internal conversion event. Following this, at around 120 s, a shift of frequency from the isomeric frequency to the ground-state frequency occurs, and is attributed to a γ decay. The half-life of $t_{1/2}^{72+} = 3.0_{-0.8}^{+1.5}$ min measured for the hydrogen-like ion in the present experiment is consistent with the value of 1.54(5) min for the neutral atom [49].

G. ^{187}Ta

A two-isomer structure similar to that observed in ^{184}Hf has been identified in ^{187}Ta. ^{187}Ta^{73+} ions were created in both the ^{190}W and ^{184}Hf ESR settings, but the $A = 187$ isobaric region was not optimized for stochastic cooling and online observation was not performed. This lack of optimization meant that observation time was decreased from ~30 s and ~1 min to <10 s and ~50 s for the ^{190}W and ^{184}Hf ESR settings respectively. Also, as this region was not monitored online, the injections were not delayed to pursue further the observation of candidate isomers. The ground state of ^{187}Ta has been observed previously [51,52]; however, its lifetime was

unknown. In some of the ^{187}Ta ground-state measurements the ions were seen to be lost from the ring. The short time scale of these losses rules out the possibility that the losses were due to electron pick-up, hence the half-life for the ground state was measured to be 2.3(6) min.

Reanalysis of the data published in Ref. [19] with different reference lines has yielded results which are in agreement with that measurement. Using the references ^{187}W^{73+} and ^{192}Os^{75+} the lower-energy isomer observed was measured to have an excitation energy of 1.793(10) MeV. In the ^{184}Hf setting, 17 ions of the ^{187}Ta^{m1} isomer were observed, most of which decayed, some as γ decays to the ground state (8 ions) while others were lost from the ring (5 ions). The latter have been attributed to β decays given the short loss time, from which a half-life of 22(9) s has been deduced. Furthermore, a higher-lying isomer was observed with a measured excitation energy of 2.933(14) MeV. In the injections, only one loss of the ion was observed and it is ambiguous as to whether this is a β decay or an atomic electron pick-up event. A half-life limit of $t_{1/2}^{73+} > 5$ min has been determined.

H. ^{186}W

Prior to this experiment a high-energy isomer was known in ^{186}W, with a measured excitation energy of 3542.8(21) keV. The half-life however was known only to be >3 ms with an upper limit of 30 s [43]. This isomer has now been observed in the ESR [Fig. 5(a)]. In Fig. 5(a) five counts are observed with a frequency difference below that of the ground state of ^{186}Ta. In principle, it could be an isomer of Li-like ^{186}Re^{72+}, but the apparent equal production cross section makes this unlikely. Moreover, measurement of the energy difference between these ions and the ^{186}W ground state gives an energy of 3560(59) keV, matching (within errors) the energy of the known isomer in ^{186}W (the references used for the energy calculation were ^{186}W^{72+} and ^{194}Pt^{75+}). Decays are observed for all ions with survival times of 7.5, 10, 15, 17.5, and 25 s. These losses from the ESR would usually be explained as being from β decay; however, this is unlikely as the ground state is stable and no β-decay events have previously been reported. Internal conversion might provide an alternative explanation since the measured ^{186}W^m ions are helium-like. Internal conversion would shift the ion such that it would have the same frequency-shift fingerprint as a β decay. A Lorentz-corrected half-life of $t_{1/2}^{72+} = 7.5_{-3.3}^{+4.8}$ s has been measured for the isomer. Our results are consistent with the >3 ms obtained previously [43], and we refer to that work for the structure interpretation. Our half-life is also in agreement with more accurate work recently obtained [53].

I. ^{190}Re

A more accurate value has been found for the known long-lived (6^-) isomer in ^{190}Re (Fig. 6). In the figure the lower-frequency peak corresponds to the ground state of the ion and the higher-frequency peak arises from an isomeric state. No decays of this isomer were observed as its half-life [3.2(2) h] is too long for decays to be seen in the ESR. The newly measured
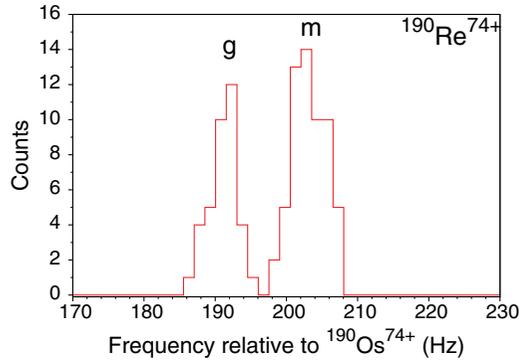
FIG. 6. (Color online) Data restricted to single-ion measurements for ^{190}Re^{74+} with ^{190}Os^{74+} ions as reference.

energy of 204(10) keV obtained using ^{190}Os^{74+} and ^{182}Hf^{71+} as references matches the published value of 210(50) [5] and an earlier ESR measurement [46] of 227(40) keV within errors.

J. ^{192}Re

A low-energy isomeric state has been newly identified in ^{192}Re (Fig. 7) through the observation of ^{192}Re^{75+} ions. It can be seen clearly that two peaks occur with different frequencies. During the experiment the isomer was seen to γ decay nine times and β decay twice, assuming that the two ion losses were not due to atomic electron capture. The observation time for
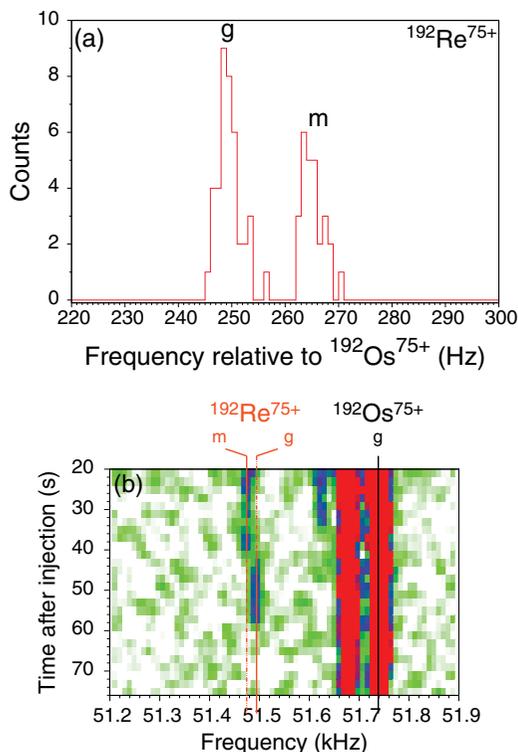
FIG. 7. (Color online) Experimental measurement of ^{192}Re^{m}. (a) Data restricted to single-ion measurements for ^{192}Re^{75+} with ^{192}Os^{75+} ions as reference. (b) A γ decay event from ^{192}Re isomer to ground state.
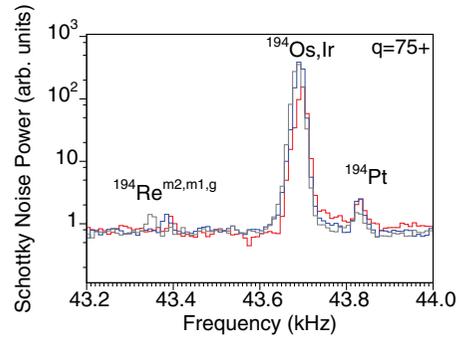
FIG. 8. (Color online) Observed ground, first, and second isomeric states in ^{194}Re, with ^{194}Pt^{75+} as a reference.

measurements of the ions was reduced to 55 s throughout a 70 s period because of ion cooling effects. In total, ^{192}Re^{m} ions were observed for 1360 s, in which 11 decays were observed, leading to a measured half-life of $t^{75+}_{1/2} = 61^{+40}_{-20}$ s. The measured excitation energy is 267(10) keV, obtained using ^{192}Os^{75+} and ^{187}W^{73+} as reference ions.

K. ^{194}Re

Recent spectroscopic studies of the neutron-rich Re isotopes identified three β-decaying states feeding levels in ^{194}Os with half-lives of 5(1), 25(8), and 100(10) s [44]. In that study it was unclear which of the parent levels were the ^{194}Re ground state and which were isomers. Using ^{194}Pt as a reference, we have observed three close-lying states around the ^{194}Re frequency region; see Fig. 8 (one ground-state ion, one first-isomer ion, and two second-isomer ions, all single ions). Using ^{194}Pt^{75+} and ^{186}W^{72+} as references, the energy of the lower isomer is measured as 285(40) keV, whilst the higher isomer has an energy of 833(33) keV. It has not been possible to associate the isomers seen here with the specific lifetimes measured previously, as neither of the isomers decays during the observation time. However, the ground-state ion decays within 20 s of the injection, and total observation time of around 6 s after cooling was measured. Therefore, it is likely that the $t^{75+}_{1/2} = 5(1)$ s β-decaying state is the ground state of ^{194}Re, as postulated in Ref. [44].

L. ^{195}Os

A low-lying $13/2^+$ isomer is expected to occur in ^{195}Os, but this has not been identified in previous experiments on this nucleus [13]. We now present evidence for the identification of a long-lived isomer which is populated more strongly than the ground state, with 73 isomeric ions and 63 ground-state ions observed. Figure 9 shows data for ^{195}Os^{76+} ions, with each count representing a frequency difference, relative to ^{187}W^{73+}. One isomeric ion was seen to γ decay and one ion was lost from the ring. With a total observation time of 3910 s, the ion loss could have been due to either β decay or atomic electron capture. Therefore the measured half-life is $t^{76+}_{1/2} = 32^{+154}_{-16}$ min, assuming the second event was an atomic electron capture, or $t^{76+}_{1/2} = 16^{+29}_{-7}$ min if the second event was a β-decay event. We
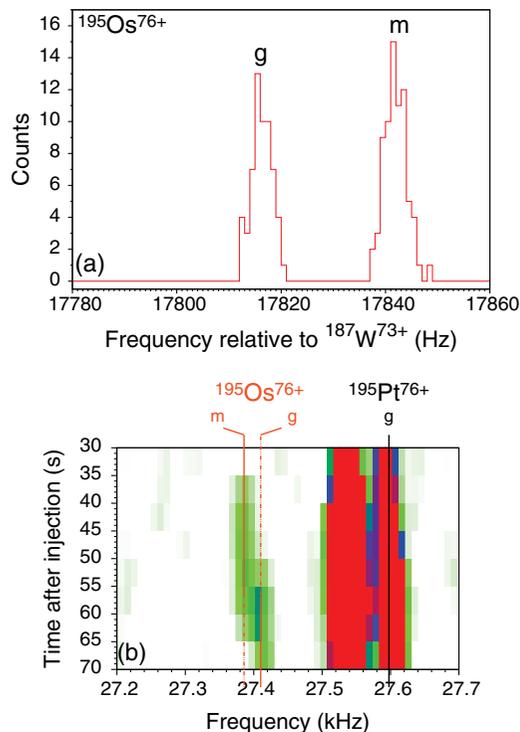
FIG. 9. (Color online) Experimental measurement of $^{195}\text{Os}^m$. (a) Data restricted to single-ion measurements for $^{195}\text{Os}^{76+}$ with $^{187}\text{W}^{73+}$ ions as reference. (b) A γ-decay from ^{195}Os isomer to ground state.

therefore suggest a half-life of $t_{1/2}^{76+} > 9$ min is appropriate. The measured excitation energy is 454(10) keV, obtained using the mass of $^{195}\text{Os}^{g,76+}$ from Ref. [46] and $^{187}\text{W}^{73+}$ as another reference.

IV. DISCUSSION

By using multi-quasiparticle (MQP) calculations, it has been possible to predict states that might give rise to isomers for comparison with experiment. The calculations give the total K^π values (where K is the angular momentum projection on the nuclear symmetry axis) and the associated energy, albeit with an uncertainty of 100–200 keV. Isomers are expected when the energy is low (for a given spin). The calculations themselves were performed using the Nilsson model for the single-particle energies together with Lipkin-Nogami pairing, self-consistent blocking, and incorporating empirical estimates of the residual interactions, according to the methodology in Refs. [54,55]. The predicted (fixed) shape parameters were taken from Möller *et al.* [56]. In some cases, comparison is also made with configuration-constrained potential-energy-surface (PES) calculations [4].

A. ^{183}Hf

Calculations predict for $^{183}\text{Hf}^m$ an energetically favoured three-quasiparticle (3QP), $K^\pi = 27/2^-$ state, made up of two quasiprotons and one quasineutron: $\pi^2\{7/2^+[404],$

$9/2^-[514]\} \otimes \nu\{11/2^+[615]\}$. This configuration is calculated to lie at 1.712 MeV, in satisfactory agreement with the experimentally measured energy of 1.464(64) MeV. The long half-life is presumably due to a large difference in K and/or spin between the isomer and possible daughter states. There is limited relevant information on lower-lying states in ^{183}Hf, but in the isotone ^{185}W, Bondarenko *et al.* [57] identify the yrast $11/2^+[651]$ band beginning, with a 197 keV bandhead and extending to the $15/2^+$ band member. Using the same energies for ^{183}Hf, and extrapolating to higher spins, it is estimated that an equivalent $21/2^+$ band member in ^{183}Hf would lie at $E^* \sim 1360$ keV. The proposed $27/2^-$ isomer would then be expected to decay by a K-forbidden $E3$ transition of about 104 keV, with a Weisskopf γ-ray half-life of about 4.5 s, a value that is close to the experimental 10-s half-life. However, such a transition would be fivefold K forbidden and therefore inhibited. For a modest reduced hindrance [7] of 20, the expected K hindrance would be about $20^5 \approx 3 \times 10^6$, making the predicted lifetime much longer than that observed. In order to explain the observed shorter lifetime, one would have to postulate that some path via intermediate-K states is available. However, without spectroscopic information the structure can only be based on theory. Such predictions do not have the necessary precision to be reliable. It should be noted that the lifetime observed here is an upper bound as internal conversion is hindered, therefore a shorter lifetime can be expected for the neutral atom.

B. ^{184}Hf

The MQP calculations for ^{184}Hf predict states which are likely to produce the observed isomers. The isomer at 1.272(1) MeV [41] has already been associated with the two-quasiproton $\{7/2^+[404], 9/2^-[514]\}$ configuration giving $K^\pi = 8^-$. The calculated energy of 1.241 MeV is very close to the experimental value of 1.272(1) MeV. This 2QP structure is well known in the lighter hafnium isotopes (Table. II). A clear candidate for the second isomer is a 4QP $K^\pi = 15^+$ state from the $\pi^2\{7/2^+[404], 9/2^-[514]\} \otimes \nu^2\{3/2^-[512], 11/2^+[615]\}$ configuration, predicted at 2.369 MeV. This matches well with the measured energy of 2.477(10) MeV. Good agreement is also found from PES calculations [4]. However, this second isomer would be expected to γ decay to a state in the rotational band associated with the 8^- isomer. Using the properties of the $K^\pi = 8^-$ rotational bands observed in ^{180}Hf and ^{182}Hf [58] as a guide to the expected rotational levels in ^{184}Hf, a K-forbidden $E3$ transition is anticipated as a possible decay from the $K^\pi = 15^+$ isomer to the 12^- state of the $K^\pi = 8^-$ rotational band, leading [7] to a partial γ-ray half-life that is much greater than the measured value of ~ 12 min. This is consistent with the fact that this isomer is only seen to β decay. Furthermore, from MQP calculations for the daughter nucleus it is possible to predict a β-decay lifetime using the selection rules set out in Ref. [59]. The most probable β decay of the $K^\pi = 15^+$ isomer is a predicted $K^\pi = 16^-$, $\pi^3\{7/2^+[404]; 9/2^-[514]; 5/2^+[402]\} \otimes \nu\{11/2^+[615]\}$ state, with the $3/2^-[512]$ quasineutron transmuting to the $5/2^+[402]$ quasiproton via changes in asymptotic

quantum numbers of $\Delta\Omega = 1$, $\Delta N = 1$, $\Delta n_z = 1$, and $\Delta\Lambda = 0$ and a decay energy of $\Delta E = 2056$ keV. Such a first-forbidden β decay has a predicted half-life in the region of 5 min $\leqslant t_{1/2} \leqslant$ 3 days, in broad agreement with the measured value of $\sim$12 min.

C. ^{186}Hf

For ^{186}Hf, a $K^\pi = 17^+$, 4QP state from the $\pi^2\{7/2^+[404], 9/2^-[514]\} \otimes \nu^2\{7/2^-[503], 11/2^+[615]\}$ configuration, calculated at 2.269 MeV, is only tentatively associated with the measured isomer at 2.968(43) MeV, since the calculated energy is considerably lower than that of the observed state. However, the energies of the Nilsson single-particle levels, particularly the $11/2^+[615]$ orbital, are not well known in this region. A similar mismatch is found with the PES calculations [4] which use a different (Woods-Saxon) potential for the single-particle energies.

The ion is not seen to decay in the ESR, therefore it is not known whether this is a γ-decaying or β-decaying state. As is the case for the 4QP isomer in ^{184}Hf, it is likely that the γ-decay partial lifetime for the ^{186}Hf isomer is long. Without more spectroscopic information, it is difficult to predict a realistic γ-decay time scale. For β decay, calculations suggest the most probable daughter state (assuming ^{186}Hf^m is $K^\pi = 17^+$) would be a $K^\pi = 16^-$, $\pi^3\{7/2^+[404], 9/2^-[514], 5/2^+[402]\} \otimes \nu\{11/2^+[615]\}$ state in ^{186}Ta, with changes of $\Delta\Omega = 1$, $\Delta N = 1$, $\Delta n_z = 0$, and $\Delta\Lambda = 1$. However, given the uncertainty in the calculations, predictions for β-decay lifetimes would be unrealistic.

The lack of an observed two-quasiparticle (8^-) state is somewhat surprising given the long lifetimes of the 8^- isomers in the lighter isotopes (see Table II). These lifetimes however, depend on several factors, including both the character of the initial two-quasiparticle states and the character and disposition of states to which they decay. For ^{186}Hf, our calculations predict that the well defined prolate character of the 8^- state will persist. Furthermore, although both Coriolis mixing and mixing between competing neutron and proton configurations play a role in the lighter isotopes [67,68], these are likely to be less relevant here. In the case of the neighbor ^{184}Hf, Krumbholz *et al.* [41] noted that the strength of its $E1$ decay to the 8^+ state of the ground-state band was in agreement with the extension of the $E1$ systematics. The variation with neutron number had been attributed to changing K mixing in the 8^+ final state [69], the evidence for which was the correlation between the strengths and the dynamic moments of inertia of the ground-state bands. However, the expected lifetime will depend not only on the transition strengths, but also on the transition energy, and for ^{186}Hf, on the presence of decay paths that might not be open in the lighter isotopes. All three factors depend, in turn, on the character of the lower-lying states: Robledo *et al.* [9] have predicted that significant changes will occur at $N = 116$ leading to a lower ground-state deformation and significantly increased gamma softness. A lower deformation would imply higher 8^+ state energies and therefore (in the absence of other effects) lower transition energies, but it also implies increased mixing, leading to the opposite effect on the lifetime. Furthermore, the

gamma softness should lead to the occurrence of low-energy vibrational bands and possibly other intrinsic states, thus opening up additional paths for the 8^- decay, substantially shortening the lifetime. Obviously, resolution of this issue depends on the identification of the purported 8^- state. Its decay hopefully would allow identification of the lower-lying structures and therefore substantiate the predicted shape changes, as well as clarifying the issue of its nonobservation in the present measurements.

D. ^{186}Ta

The high level density in odd-odd ^{186}Ta can be seen from the calculated 2QP states in Table III. In addition to β^- decay [49], the isomer is seen to γ decay (Fig. 6) and the Weisskopf estimate of the partial γ-ray half-life should be of the order of minutes, implying either $M3$ or $E4$ multipolarity (for a pure spin-trap isomer, with no K forbiddenness). However, Xu *et al.* [49] identify no additional β-delayed gamma rays in the isomer decay, compared to the ground-state decay [70], and it is not clear whether it is the isomer or the ground state which has the higher spin value. We suggest that the higher-spin state is the ground state, on account of its longer half-life of 10.5 min [70,71]. It is then possible to understand our new half-life data for the isomer in a simple way: We consider that the 336(20) keV isomer may have a direct $M3$ or $E4$ decay branch to the ground state, with a theoretical neutral-atom conversion coefficient of $\alpha \sim 1$ [47]. Our one-electron ions of ^{186}Ta^{72+} would then have a significantly (though not greatly) extended half-life, which is compatible with the observed values of 3 min in the ESR and 1.5 min for the neutral atom [49]. This analysis implies that the ground state has the same parity as the isomer, with three or four additional units of spin. Ignoring the specific calculated energies, which have considerable uncertainties, pairs of states can be found in Table III which satisfy these criteria (such as 3^- and 6^-) but additional spectroscopic data are needed if detailed assignments are to be made.

TABLE III. 2QP states in ^{186}Ta calculated with the method of Jain *et al.* [54] excluding residual energy splittings. The energy-unfavored K^π couplings are included in parentheses.

K^π	ν	π	E^* (keV)
$(9^+)\,\mathbf{2^+}$	$11/2^+[615]$	$7/2^+[404]$	0.00
$\mathbf{10^-}\,(1^-)$	$11/2^+[615]$	$9/2^-[514]$	124
$\mathbf{8^+}\,(3^+)$	$11/2^+[615]$	$5/2^+[402]$	221
$(7^-)\,\mathbf{0^-}$	$7/2^-[503]$	$7/2^+[404]$	227
$(5^-)\,\mathbf{2^-}$	$3/2^-[512]$	$7/2^+[404]$	267
$\mathbf{8^+}\,(1^+)$	$7/2^-[503]$	$9/2^-[514]$	352
$(4^-)\,\mathbf{3^-}$	$1/2^-[510]$	$7/2^+[404]$	364
$(6^+)\,\mathbf{3^+}$	$3/2^-[512]$	$9/2^-[514]$	392
$\mathbf{6^-}\,(1^-)$	$7/2^-[503]$	$5/2^+[402]$	449
$(4^-)\,\mathbf{1^-}$	$3/2^-[512]$	$5/2^+[402]$	487
$\mathbf{5^+}\,(4^+)$	$1/2^-[510]$	$9/2^-[514]$	488
$\mathbf{3^-}\,(2^-)$	$1/2^-[510]$	$5/2^+[402]$	585
$(6^+)\,\mathbf{5^+}$	$11/2^+[615]$	$1/2^+[411]$	659
$\mathbf{8^-}\,(1^-)$	$9/2^-[505]$	$7/2^+[404]$	967
$(9^+)\,\mathbf{0^+}$	$9/2^-[505]$	$9/2^-[514]$	1092

E. ^{187}Ta

MQP calculations performed for the new isomers in ^{187}Ta were initially found to give energies very different from the experimentally measured values. As with the isomer in ^{186}Hf, the Nilsson model did not predict the single-particle levels correctly for ^{187}Ta. However, the neutron single-particle orbitals are known experimentally for the close isobar of ^{187}W and it is possible to incorporate the energies of these known neutron orbitals into the calculation for ^{187}Ta, resulting in much better agreement between the calculated and measured isomer energies. The first isomer at 1.789(13) MeV can be associated with a $K^\pi = 27/2^+$, 3QP state from the $\pi\{9/2^-[514]\} \otimes \nu^2\{7/2^-[503], 11/2^+[615]\}$ configuration, calculated to lie at 1.508 MeV. The higher lying isomer at an energy of 2.935(14) MeV can be associated with the $K^\pi = 41/2^+$, 5QP configuration $\pi^3\{7/2^+[404], 9/2^-[514], 5/2^+[402]\} \otimes \nu^2\{9/2^-[505], 11/2^+[615]\}$, calculated at 2.710 MeV. The problem with the standard Nilsson-model parameters in the neutron-rich region shows the need for systematic analysis of single-particle energies, but this in turn requires additional experimental data.

A notable feature of ^{187}Ta^{m2} is that the half-life (>5 min) is greater than the half-life of the ground state (2.3 min) because of the constraints on the spin and parities of the parent and daughter states and the energy between them. The most probable daughter state could be the $K^\pi = 43/2^+$, π^4 {7/2$^+$[404], 9/2$^-$[514], 5/2$^+$[402], 11/2$^-$[505]} $\otimes \nu\{11/2^+[615]\}$ configuration in ^{187}W. This would be an allowed transition with changes of $\Delta\Omega = 1$, $\Delta N = 0$, $\Delta n_z = 0$, and $\Delta\Lambda = 0$. The associated decay energy of 4.4 MeV gives an estimated β-decay lifetime of 10 min $< t_{1/2} <$ 7 days.

F. ^{192}Re

The ground-state β decay of ^{192}Re populates the 2^+ and 0^+ states in ^{192}Os [42]. Coupled with the longer partial β decay half-life of the isomer, this suggests that the ground state of ^{192}Re is a low-spin state and the isomer is of significantly higher spin. Table IV shows PES calculations for the low-energy states. Here the shape polarization induced by specific quasiparticles has been taken into account. The 267(10) keV isomer is seen to γ decay and the Weisskopf half-life should be of the order of minutes, implying either a low-energy $E3$ ($\sim$75 keV) or an $M3$ ($\sim$150 keV) transition.

Additional spectroscopic data are required to pin down the structure of this isomer. We note that the neutral-atom half-life, due to electron conversion, will be considerably shorter than the bare-ion half-life of approximately 60 s measured here.

G. ^{194}Re

The fastest transition observed in the spectroscopic analysis of ^{194}Re (5(1) s) was interpreted earlier as feeding an excited 0^+ state in the daughter ^{194}Os [44]. In comparison with the decay times measured from the ESR, the lowest-energy state seen in ^{194}Re, i.e., the ground state, fits this lifetime. The second fastest transition [25(8) s] was thought to be feeding a possible 11^- state, and the slowest transition [100(10) s] was thought to feed a possible 6^+ state [44]. It has not been possible to assign a measured β-decaying state to an isomer energy measured in the ESR because of lack of decay information. Possible states are discussed in Ref. [44].

H. ^{195}Os

In Ref. [13] the observed γ cascade is assumed to feed a neutron $13/2^+[606]$ state, sitting above a neutron $3/2^-[501]$ ground state. Direct decay from $13/2^+$ to $3/2^-$ requires an $E5$ transition, therefore a long lifetime is expected. As the present isomer is observed to γ decay this presumably takes place through an intermediate state, possibly a member of the rotational band built on the $3/2^-$ state, similar to the situation in ^{193}Os [72]. It would appear that the isomer ($t_{1/2} > 9$ min) is more stable to β decay than the ground state ($t_{1/2} \sim 9$ min [12]). In considering β decay, the daughter state would have to be of similar spin to the $13/2^+[606]$ state. The obvious candidate for this is the $11/2^-[505]$ isomer in ^{195}Ir [73]; a β-decay transition to this would be first forbidden with $\Delta E \sim$ 2.5 MeV [59], giving a β-decay lifetime of the order of minutes to days. Given this, it remains possible that the loss of a ^{195}Os^m ion from the ESR is due to β decay, as the atomic electron capture and predicted β-decay lifetimes are comparable.

V. REVIEW OF MULTI-QUASIPARTICLE CALCULATIONS

In this section, comparison is made between the experimental energies for even-even hafnium four-quasiparticle states and the results of MQP calculations, as illustrated in

TABLE IV. 2QP states in ^{192}Re from PES calculations. The energy-unfavored K^π couplings are included in parentheses.

K^π	ν	π	E^* (keV)	Deformation		
				β_2	γ	β_4
(7^-) **2$^-$**	$9/2^-[505]$	$5/2^+[402]$	0.0	0.152	0.468	-0.060
(6^+) **3$^+$**	$3/2^-[512]$	$9/2^-[514]$	62	0.151	-25.034	-0.046
8$^+$ (3^+)	$11/2^+[615]$	$5/2^+[402]$	173	0.148	0.307	-0.056
(9^+) **0$^+$**	$9/2^-[505]$	$9/2^-[514]$	177	0.150	-0.132	-0.058
10$^-$ (1^-)	$11/2^+[615]$	$9/2^-[514]$	199	0.141	1.295	0.046
5$^+$ (4^+)	$1/2^-[510]$	$9/2^-[514]$	523	0.136	0.463	-0.043
8$^+$ (1^+)	$7/2^-[503]$	$9/2^-[514]$	597	0.147	0.391	-0.057
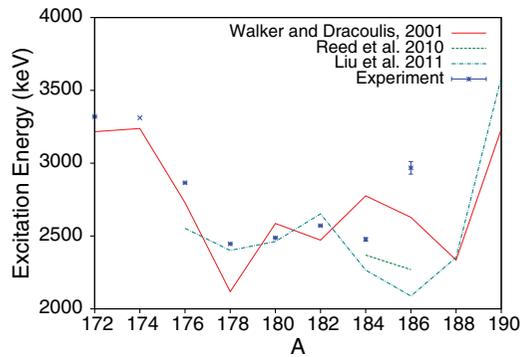
FIG. 10. (Color online) Variation of four-quasiparticle energies with mass number for even-even hafnium isotopes. The experimental data are from Ref. [5] and the present work, while the calculations are from Refs. [4,7,19].

Fig. 10. The experimental values now extend from ^{172}Hf to ^{186}Hf [7,19]. Using the Nilsson model with blocked-BCS pairing [54], a systematic set of calculations was carried out by Walker and Dracoulis [7], ranging from ^{172}Hf to ^{190}Hf. The mean deviation was 185 keV compared to the then-known experimental energies, i.e., ^{172}Hf to ^{182}Hf, without minimization of the deviation by parameter adjustments. For ^{184}Hf and heavier isotopes, these calculations have served as predictions, which were part of the motivation for the present experimental studies.

Compared to the measured ^{184}Hf isomer energy of 2477(10) keV, the predicted energy [7] of 2776 keV was 300 keV too high. This was for a $K^\pi = 17^+$ configuration, the same as that given above for ^{186}Hf (Sec. IV C). However, new calculations [19], which include Lipkin-Nogami pairing, favor a $K^\pi = 15^+$ configuration (given in Sec. IV B) where the energy is calculated to be 2369 keV, i.e., 110 keV too low. The $K^\pi = 15^+$ assignment is supported by recent Woods-Saxon-Strutinsky PES calculations [4]. While further experimental information is needed to substantiate the ^{184}Hf spin and parity assignments, the present agreement with calculations is considered to be satisfactory.

For ^{186}Hf the situation is much less clear. The different calculations all predict the same $K^\pi = 17^+$ configuration for the isomer (given in Sec. IV C) but all the corresponding energies are more than 300 keV too low. The isomer energies in ^{187}Ta, an isotone of ^{186}Hf, are also substantially underpredicted [19] unless the neutron single-particle energies are adjusted—in that case to give better agreement for known single-particle states in ^{187}W. Therefore, for ^{186}Hf, it may be that the $K^\pi = 17^+$ assignment is correct, but that a systematic reevaluation of the model parameters is required for the neutron-rich region, in order to obtain the correct single-particle energies. It is hoped that isomer studies such as those presented here will motivate further theoretical work of this kind.

An important part of obtaining the correct single-particle energies is the treatment of the nuclear shape. The neutron-rich hafnium isotopes are associated with a predicted prolate-oblate shape transition close to $N = 116$, corresponding to ^{188}Hf [8,9]. Despite this, PES calculations [4] indicate that high-K configurations stabilize prolate shapes, and prolate high-K

isomers are still expected to persist, at least in ^{188}Hf. It is planned that this will be tested experimentally in the ESR. Furthermore, with isomer decay studies it should be possible to populate and identify low-spin states for comparison with detailed structure calculations [74].

VI. SUMMARY

The aim of this experiment was to access neutron-rich exotic isomers; to this end the experiment succeeded [19]. Initially the experiment was designed to search for predicted long-living isomers in ^{184,186}Hf isotopes [7] and a possible isomer in ^{190}W, through projectile fragmentation of a ^{197}Au beam. By operating the ESR in SMS mode it was possible to directly observe isomers and ground states with lifetimes greater than a few seconds. The experiment allowed for many different nuclei to be injected into the ESR. This enabled not only investigations into the ^{184,186}Hf and ^{190}W isotopes, but also other nuclei around the same region of the nuclear chart. For example, online observations of $A = 184$ ions enabled the detection of ^{184}Hf isomers, which were observed in real time during the experiment. This confirmed the existence of a previously measured 2QP long-living isomer [41] and a predicted 4QP long-lived isomer [7]. All the other isomers discovered in the experiment were found offline. Isomers were observed in nuclei with $Z = 72$ to $Z = 76$ and $N = 111$ to $N = 119$, with lifetimes ranging from seconds to greater than minutes, and excitation energies from ~ 200 keV to ~ 3 MeV. Some results obtained relate to previously known isomers, ^{184}Hf^{m1}, ^{186}Ta^m, ^{186}W^m, ^{190}Re, and ^{194}Re^{m1,m2}, with the measurements adding to experimental knowledge of the states. Other isomers are completely new discoveries, such as ^{183,186}Hf^m, ^{184}Hf^{m2}, ^{187}Ta^{m1,m2}, ^{192}Re^m, and ^{195}Os^m.

It has been possible to use multi-quasiparticle calculations to predict states that would lead to isomers. For the high-spin high-energy isomers there are generally very few candidate configurations, making interpretation and assignment of the isomeric structure relatively straightforward. However, the low-energy isomers have many candidate configurations and, in the absence of solid spectroscopic data, interpretation of the low-lying isomeric structure remains difficult. For ^{192}Re PES calculations were performed to account for configurations having different shapes. The results pave the way for new spectroscopic experiments to examine the structure of these nuclei in more detail.

Evidence for candidate isomers in ^{185}Ta, ^{188}Ta, ^{185}W, ^{191}Re, and ^{195}Ir, has also been obtained and will be the subject of further analysis and experiments. Such measurements are planned using the ESR with fragmentation of ^{197}Au and ^{208}Pb beams, where ^{186}Hf and ^{188}Hf isomers are the main focus. Furthermore, a novel, highly-sensitive, resonant Schottky detector has been developed [75] that allows accurate determination of revolution frequencies of single stored ions within a few tens of milliseconds. The latter will enable the study of shorter-lived isomeric states than those measured with the present experiment.

[1] S. Aberg, Nucl. Phys. A **306**, 89 (1978).

[2] P. M. Walker and G. D. Dracoulis, Nature (London) **399**, 35 (1999).

[3] F. R. Xu, P. M. Walker, and R. Wyss, Phys. Rev. C **62**, 014301 (2000).

[4] H. L. Liu, F. R. Xu, P. M. Walker, and C. A. Bertulani, Phys. Rev. C **83**, 067303 (2011).

[5] G. Audi, O. Bersillon, J. Blachot, and A. H. Wapstra, Nucl. Phys. A **729**, 3 (2003).

[6] J. Van Klinken, W. Z. Venema, R. V. F. Janssens, and G. T. Emery, Nucl. Phys. A **339**, 189 (1980).

[7] P. M. Walker and G. D. Dracoulis, Hyperfine Interact. **135**, 83 (2001).

[8] P. D. Stevenson, M. P. Brine, Zs. Podolyak, P. H. Regan, P. M. Walker, and J. R. Stone, Phys. Rev. C **72**, 047303 (2005)

[9] L. M. Robledo, R. Rodríguez, and P. Sarriguren, J. Phys. G **36**, 115104 (2009).

[10] J. Benlliure, K.-H. Schmidt, D. Cortina-Gil, T. Enqvist, F. Farget, A. Heinz, A. R. Junghans, J. Pereira, and J. Taieb, Nucl. Phys. A **660**, 87 (1999).

[11] R. Grzywacz *et al.*, Phys. Lett. B **355**, 439 (1995).

[12] M. Caamaño *et al.*, Eur. Phys. A **23**, 201 (2005).

[13] S. J. Steer *et al.*, Phys. Rev. C **84**, 044313 (2011).

[14] B. Sun *et al.*, Eur. Phys. J. A **31**, 393 (2007).

[15] Yu. A. Litvinov *et al.*, Nucl. Phys. A **756**, 3 (2005).

[16] H. Geissel *et al.*, Nucl. Instrum. Meth. B **70**, 286 (1992).

[17] A. E. Stuchbery, G. D. Dracoulis, T. Kibedi, A. P. Byrne, B. Fabricius, A. R. Poletti, G. J. Lane, and A. M. Baxter, Nucl. Phys. A **641**, 401 (1998).

[18] Zs. Podolyák *et al.*, Phys. Lett. B **632**, 203 (2006).

[19] M. W. Reed *et al.*, Phys. Rev. Lett. **105**, 172501 (2010).

[20] B. Franzke, Nucl. Instrum. Meth. B **24-25**, 18 (1987).

[21] O. Klepper *et al.*, Nucl. Instr. Meth. B **70**, 427 (1992).

[22] T. Winkler *et al.*, Nucl. Phys. A **626**, 458c (1997).

[23] F. Nolden *et al.*, Nucl. Instrum. Meth. A **441**, 219 (2000).

[24] T. Radon *et al.*, Nucl. Phys. A **677**, 75 (2000).

[25] F. Bosch, J. Phys. B **36**, 585 (2003).

[26] M. Steck *et al.*, Phys. Rev. Lett. **77**, 3803 (1996).

[27] H. Poth, Phys. Rep. **196**, 135 (1990).

[28] H. Geissel *et al.*, Nucl. Phys. A **746**, 150c (2004).

[29] M. Hausmann *et al.*, Nucl. Instrum. Meth. A **446**, 569 (2000).

[30] B. Sun *et al.*, Phys. Lett. B **688**, 294 (2010).

[31] Yu. A. Litvinov *et al.*, Phys. Lett. B **573**, 80 (2003).

[32] B. Schlitt *et al.*, Hyperfine Interact. **99**, 117 (1996).

[33] B. Schlitt, Ph.D. Thesis, University of Heidelberg, 1997.

[34] B. Franzke, H. Geissel, and G. Münzenberg, Mass Spectrom. Rev. **27**, 428 (2008).

[35] U. Schaaf, Ph.D. Thesis, Johann-Wolfgang-Goethe-Universität Frankfurt, 1991 (unpublished).

[36] Yu. A. Litvinov and F. Bosch, Rep. Prog. Phys. **74**, 016301 (2011).

[37] Yu. A. Litvinov *et al.*, Hyperfine Interact. **173**, 55 (2006).

[38] B. Sun *et al.*, Chin. Phys. C **33** (Suppl. 1), 161 (2009).

[39] N. R. Johnson and W. N. Bishop, Nucl. Phys. **69**, 131 (1965).

[40] P. E. Haustein, E. M. Franz, S. Katcoff, N. A. Morcos, H. A. Smith, and T. E. Ward, Phys. Rev. C **14**, 645 (1976).

[41] K. Krumbholz *et al.*, Z. Phys. A **351**, 11 (1995).

[42] R. B. Firestone, *Table of Isotopes* (John Wiley and Sons, New York, 1996).

[43] C. Wheldon *et al.*, Phys. Lett. B **425**, 239 (1998).

[44] N. Al-Dahan *et al.*, Phys. Rev. C **85**, 039904(E) (2012).

[45] K.-H. Schmidt, C.-C. Sahm, K. Pielenz, and H.-G. Clerc, Z. Phys. A **316**, 19 (1984).

[46] I. J. Cullen, Ph.D. Thesis, University of Surrey, 2010.

[47] T. Kibédi, T. W. Burrows, M. B. Trzhaskovskaya, P. M. Davidson, C. W. Nestor Jr. *et al.*, Nucl. Instrum. Meth. A **589**, 202 (2008).

[48] Y. Shuanggui, Y. Weifan, Li Zongwei, He Jianjun, Ma Taotao, F. Keming, S. Shuifa, G. Zaiguo, P. Qiangyan, C. Zhantu, G. Tianrui, M. Wantong, Su Denggui, Xu Yanbing, G. Junsheng, L. Hongye, S. Lijun, Z. Zhizheng, and Ma Huifan, Phys. Rev. C **57**, 1506 (1998).

[49] Y. Xu, W. Yang, S. Yuan, Y. Niu, H. Ding, X. Wang, L. Zhao, P. Wang, and H. Li, J. Phys. Soc. Jpn. **73**, 2588 (2004).

[50] M. W. Reed *et al.*, J. Phys. Conf. Ser. **381**, 012058 (2012).

[51] Zs. Podolyák *et al.*, in *Proceeding of the 2nd International Conference on Fission and Properties of Neutron-Rich Nuclei*, edited by J. H. Hamilton, W. R. Phillips, and H. K. Carter (World Scientific, Singapore, 1999).

[52] N. Alkhomashi *et al.*, Phys. Rev. C **80**, 064308 (2009).

[53] G. J. Lane *et al.* (private communication).

[54] K. Jain *et al.*, Nucl. Phys. A **591**, 61 (1995).

[55] F. G. Kondev, G. D. Dracoulis, A. P. Byrne, T. Kibédi, and S. Bayer, Nucl. Phys. A **617**, 91 (1997).

[56] P. Moller, J. R. Nix, W. D. Myers, and W. J. Swiatecki, At. Data Nucl. Data Tables **59**, 185 (1995).

[57] V. Bondarenko *et al.*, Nucl. Phys. A **762**, 167 (2005).

[58] R. D'Alarcao *et al.*, Phys. Rev. C **59**, R1227 (1999).

[59] G. Alaga, Nucl. Phys. **4**, 625 (1957).

[60] D. M. Cullen, D. E. Appelbe, A. T. Reed, C. Baktash, I. Y. Lee, and A. O. Macchiavelli, Phys. Rev. C **60**, 057303 (1999).

[61] P. M. Walker, G. D. Dracoulis, A. Johnston, and J. R. Leigh, Nucl. Phys. A **293**, 481 (1977).

[62] T. L. Khoo, F. M. Bernthal, J. S. Boyno, and R. A. Warner, Annual Report, Michigan State University Cyclotron Laboratory, 1974 (unpublished), p. 65.

[63] T. L. Khoo, F. M. Bernthal, R. A. Warner, G. F. Bertsch, and G. Hamilton, Phys. Rev. Lett. **35**, 1256 (1975).

[64] T. E. Ward and Y. Y. Chu, Phys. Rev. C **12**, 1632 (1975).

[65] D. L. Bushnell, D. J. Buss, and R. K. Smither, Phys. Rev. C **10**, 2483 (1974).

[66] T. E. Ward and P. E. Haustein, Phys. Rev. C **4**, 244 (1971).

[67] G. D. Dracoulis *et al.*, Phys. Lett. B **635**, 200 (2006).

[68] G. D. Dracoulis *et al.*, Phys. Rev. C **79**, 061303 (2009).

[69] P. M. Walker, G. D. Dracoulis, A. P. Byrne, T. Kibedi, and A. E. Stuchbery, Phys. Rev. C **49**, 1718 (1994).

[70] B. P. Pathak, K. S. N. Murty, S. K. Mukherjee, and S. C. Gujrathi, Phys. Rev. C **1**, 1477 (1970).

[71] S. C. Gujrathi and S. K. Mark, Can. J. Phys. **51**, 241 (1973).

[72] D. D. Warner, W. F. Davidson, H. G. Börner, R. F. Casten, and A. I. Namenson, Nucl. Phys. A **316**, 13 (1979).

[73] K. J. Hofstetter and P. J. Daly, Nucl. Phys. A **106**, 382 (1967).

[74] K. Nomura, T. Otsuka, R. Rodríguez-Guzmán, L. M. Robledo, and P. Sarriguren, Phys. Rev. C **84**, 054316 (2011).

[75] F. Nolden *et al.*, Nucl. Instrum. Meth. A **659**, 69 (2011).